Proceedings of the Twenty-Ninth International Pump Users Symposium
October 1- 3, 2013, Houston, Texas

IMPLEMENTATION AND LONG-STEP SENSORLESS CONTROL OF PERMANENT MAGNET SYNCHRONOUS MACHINES (PMSM) FOR SUBSEA APPLICATIONS

Costin Ifrim
Manager of Subsea Systems
FMC Technologies
Direct Drive Systems
Fullerton, CA, USA

Harald Bjorn Ulvestad
Technology Expert, Power Systems
FMC Kongsberg Subsea AS
Asker, Norway

Terje Hollingsæter
Chief Engineer
FMC Kongsberg Subsea AS
Asker, Norway

Lorenz Schneider
Development Engineer Subsea Pumps
Sulzer Pumps Ltd.
Winterthur, Switzerland

Shanbao Cheng
ECM Engineer
FMC Technologies
Direct Drive Systems
Fullerton, CA, USA

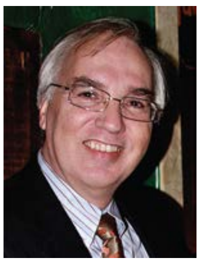

Dr. Costin Ifrim *leads the development of subsea motor technology for Direct Drive Systems, a business unit of FMC Technologies. An expert in the design of high-speed, high-power motors and generators for a variety of applications, including wind generation and utility/grid power conversion, he has established electromagnetic design methodologies based on analytical and 3D FEA. He has seven issued patents in the power electrical engineering field and has published more than 70 technical papers. Dr. Ifrim holds a Ph.D. in Power Electrical Engineering and a M.S. in Electrical and Electronics Engineering from "Politehnica" University Bucharest, Romania and University Pierre et Marie Curie –Paris, France.*

ABSTRACT

By design, the operation of a large 3MW permanent magnet motor-driven pump system has the potential to improve system efficiency and reliability to lower operator costs. Subsea electrical system design and motor performance must be predictable and validated prior to deployment.

Critical elements of this system include successful remote start-up and step up–step down transformers. A number of different strategies for open loop control systems were analyzed. One of these models is presented in this paper. The model has been recently validated by the test data obtained from a 3.2MW-rated subsea motor-driven pump system at the Sulzer Pumps Ltd. facilities in Leeds, United Kingdom.

INTRODUCTION

One of the main challenges in using an open loop long-step start-up system consists in the incertitude of the initial position of the permanent magnet rotor relative to the stator's initial excitation. When step up–step down transformers are used, their sizing, as a function of the starting frequency and the initial motor current consumption, is a key factor in the system optimization design.

From a subsea multiphase boosting perspective the permanent magnet motor provides the following advantages:

- The larger liquid-filled gap between rotor and stator of a PMSM results in significantly lower drag losses and thus allows operation at higher speeds than a liquid-filled asynchronous machine. This enables multiphase boosting at high rates and high pressure rise.

- The torque characteristics of the PMSM, controlled with vector control, is optimally suited for multiphase boosting application as it enables generation of high pressure rise over a wide range of gas void fractions (GVF).

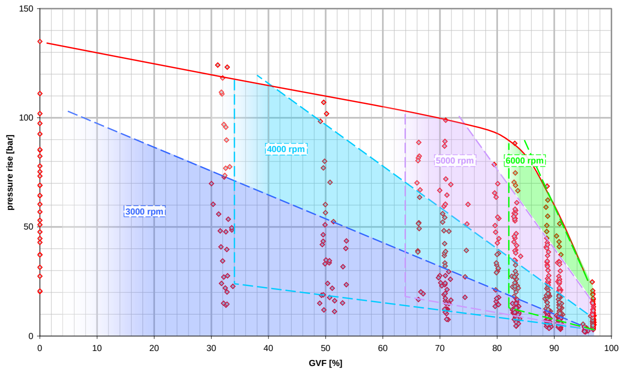

Figure 1
Operating range of a qualified 3.2 MW helico-axial multiphase subsea pump

Due to the different behavior of the incompressible liquid phase and the compressible gas phase, multiphase boosting requires:

- High torque at lower speeds
- Reduced torque at higher speeds

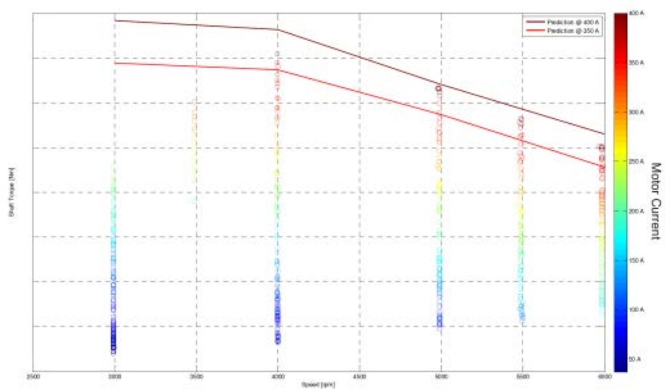

Figure 2
Measured shaft torque

Requirements from a Pump Perspective

The motor start-up strategy for sensorless PMSM requires sufficient robustness against variation in the start-up load curve. In multiphase boosting, the load absorbed by the pump is strongly affected by different factors:

- Friction loss in bearings and dynamic seals
- Speed
- Process conditions (mainly GVF)

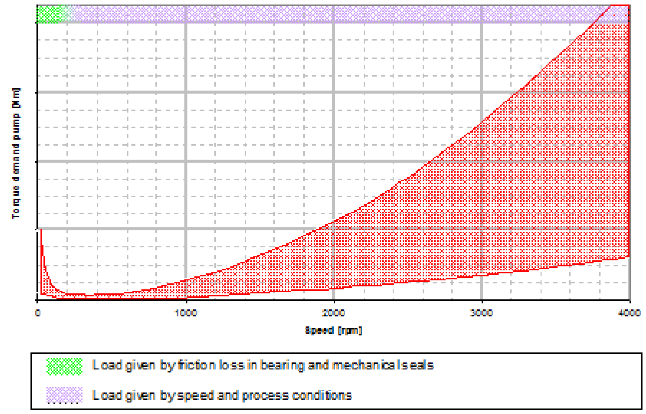

Figure 3
Speed dependent torque load

As a result, the load required during start-up is not monotonically increasing with speed and exhibits large variations.

SYSTEM SIMULATIONS

System consideration

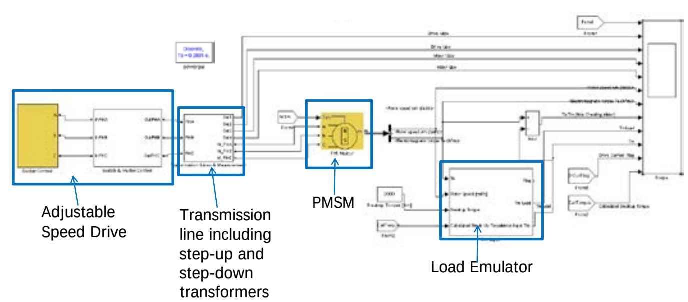

Figure 4
Top level system model of the long-step

Figure 4 represents the system layout, from left to right in the order of connections: the drive, the "topside" transformer, the umbilical simulator, the "subsea" transformer and the subsea permanent magnet motor-driven pump.

Start-up Procedure

For this paper, we selected the start-up algorithm represented in Figure 5. This algorithm is not a function of, or dependent on, the rotor position or its initial angle.

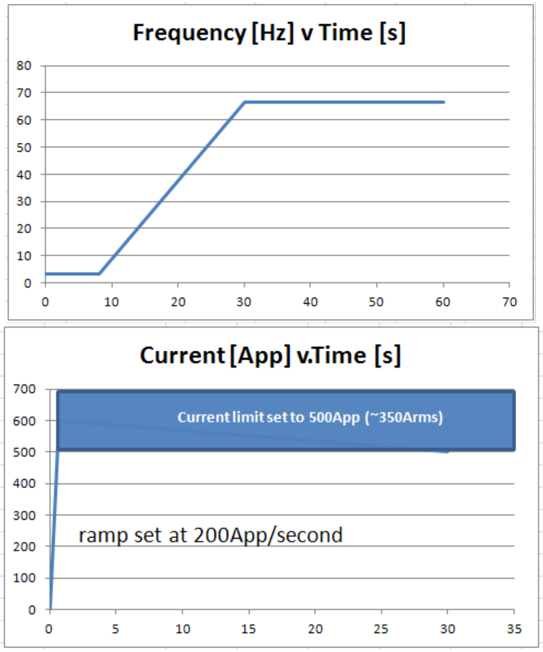

Figure 5
Start-up frequency (top) and current (bottom) profiles

Motor Load Model

One major challenge to accurately simulate the system behavior was represented by the modeling of the pump's torque-speed characteristic as the mechanical load curve of the PMSM. Figure 6 represents the load – rpm curve for the rotor shaft. In steady state operation, the shaft operational point is in the first quadrant, for positive speed and torque, while the load is represented in the fourth quadrant since it represents a negative torque for a given positive shaft speed.

If there is a slight rotor oscillation, (temporarily negative shaft speed and shaft torque – third quadrant), then the mechanical load shifts in the second quadrant. It has to be noted that there is only one sequence of overcoming the breakout torque. Once this is exceeded and the speed breaks out from zero (blue line) the potential oscillating rotor position will follow the load marked by the red line.

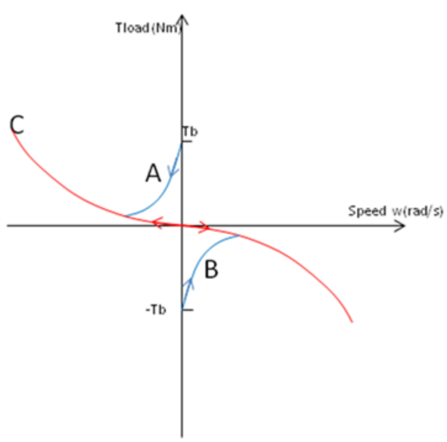

Figure 6
Pump load – speed characteristics
Blue is the breakout torque, red is for post-breakout conditions

Figure 7, below, is a representation of one of those cases where the rotor has a slight oscillation during the start-up.

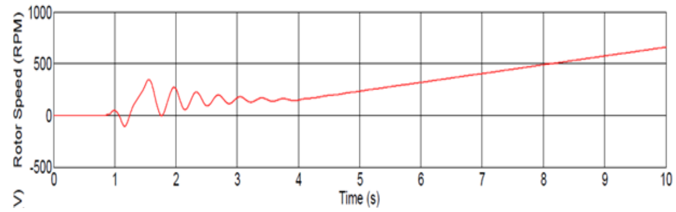

Figure 7
Rotor start-up speed, stabilized at ~200 rpm and ramped up

TEST SETUP

Figure 8 is a representation of the test setup. From left to right there is the Drive (VSD), the transformer that emulates the "topside" unit, the umbilical simulator, the transformer that emulates the "subsea" unit and the motor-pump assembly.

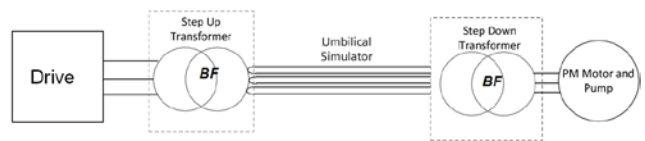

Figure 8
Test system and boosting factors' identifications (BF)

The boosting factor (BF) requires some special considerations since it defines the size of the transformer. This factor is defined by the following requirements:

- to compensate the voltage drop (or IR compensation) of the long line under low start-up frequency
- to mitigate the transient increased current during initial start-up process

System Data

On the topside transformer and its high voltage terminal (see Figure 8) the following numerical values were implemented:

A = 0.154 m^2 (238.8 inch^2)
$N_{HV} = 454/\sqrt{3}$ = 262 turns at 26220V (-Y)

On the identical transformer, emulating the "subsea" side, the number of turns on the low voltage/motor side is:

N_{LV} = 138 turns at 13800V (-Y)

Figure 9 is a picture of the motor pump assembly in the test pool at Leeds, UK.

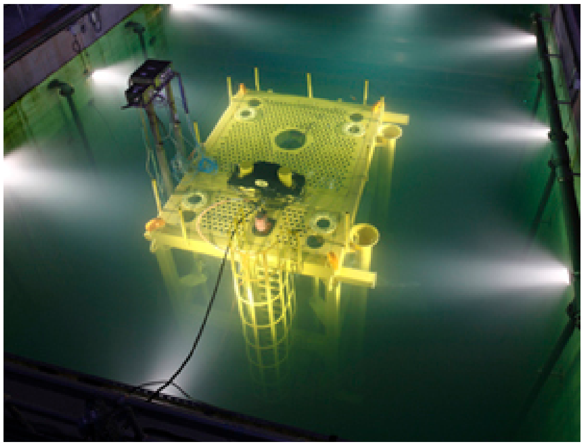

Figure 9
Sulzer Pumps' purpose-built test facility in
Leeds, United Kingdom

COMPARATIVE SIMULATIONS AND TEST RESULTS

Motor Characterization - "Fingerprint" Tests

Purpose and Methodology

The purpose of performing these tests is to validate, through test results, that a permanent magnet synchronous motor will require a relative constant electrical power at its terminals regardless of the initial position of the rotor.

Challenges and Mitigation

In a sensorless start-up control system, the position of the rotor is unknown. This is perceived as a potential challenge based on a commonly assumed assertion that, if the rotor fails to synchronize with the rotating magnetic field of the stator, there will be an increased demand of electric power at the motor terminals.

A number of randomly selected start-ups (minimum 10) have been selected so that the rotor initial position will be assumed at different angles, including those particular cases when there is a reversal present during the start-up.

Simulation and Test Results

Simulation

Figure 10 is a representation of the family of the current RMS values resultant from start-up simulations performed in increments of 30 degrees. The 275 A RMS corresponds to the value of 390A peak to peak.

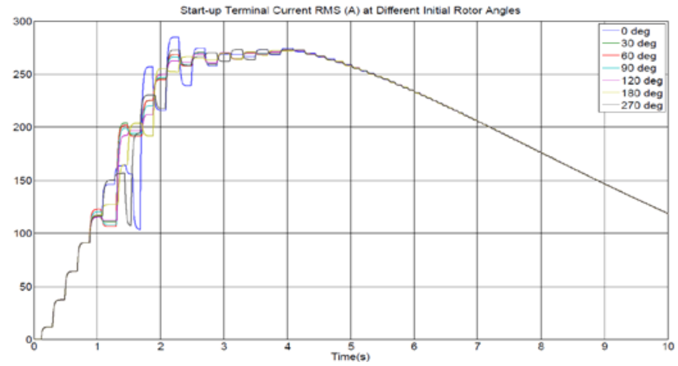

Figure 10
Terminal current (RMS) for different initial rotor angles

Test Results

We selected four of the start-up terminal current data recordings, three presented in Figure 11 and one, separate, in Figure 12. Please note that the peak current values are closely matching the simulation predictions of about 390 App.

Figure 12 requires some additional attention. It should be noted that there is a change in the sequence of the three phase currents. This is marked by the two ovals. The change occurs when the rotor reverses its rotation during the start-up process. This is consistent with the representation that was selected for the graphic in Figure 10.

Note:

The representation in Figure 10 is for current (Amps) RMS values, selected in this way to accommodate the entire family of start-up initial rotor angles.

Figures 11 and 12 represent the captures of the tested currents for a few start-up profiles. The matching between the simulated and predicted values is reflected by the markers with dotted lines.

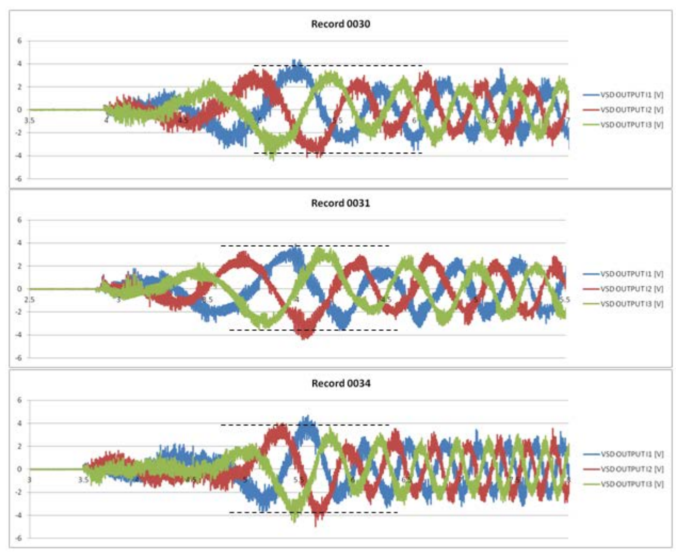

Figure 11
"Fingerprint" test results
Dotted line represents the simulated data

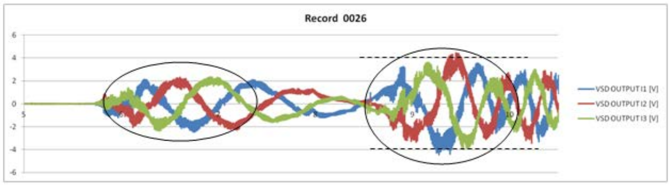

Figure 12
"Fingerprint" test results for a rotor with oscillating direction; dotted line represents the simulated data

Figure 12 is an example of those situations when the rotor has an oscillation, backward and forward. In the marked area, left, the sequence of the three phases is blue-red-green (reversed sequence) while the direct one is green-red-blue as in Figure 11.

Note: The current "fingerprint" resulting from a backwards start-up does not exceed the predicted threshold values and in fact is contained within the same peak-to-peak values as the ones observed during the forward start-up (Figure 11).

Magnetic Flux Determination across Transformers

Purpose and Methodology

The most critical requirement for the system sizing is the excitation of the transformers. The transformers must be sized such that, during transients, the magnetic core will not saturate.
The scope of the following simulations and tests is to validate the magnetic design for the long-step out system.

Data inputs: terminal voltages as function of time

$$u_t(t) = -N \cdot \frac{d\emptyset_t}{dt} \tag{1}$$

where: u_t is transformer's terminal voltage, N is the number of turns

$\frac{d\emptyset_t}{dt}$ is time derivative of the magnetic flux in transformers core leg

Magnetic flux density determination:

From (1) the magnetic flux is calculated:

$$\emptyset_t = \int d\emptyset_t = -\frac{1}{N} \cdot \int u_t(t)dt + \mathrm{C} \tag{2}$$

Where "C" is a constant required to be applied as a corrective factor against a possible bias component resulting from the indefinite integral. The bias component has no physical meaning and it has to be applied after the initial transient ends.

The values of the magnetic flux densities are obtained:

$$B = -\frac{1}{A \cdot N} \cdot \int u_t(t)dt \tag{3}$$

where A is transformer's core leg cross section

Simulation and Test Results

Simulation

Figure 14 represents one of the test results processed according to the equations 1-3. The raw data consists in voltage function in time; the processed data is the magnetic flux in the topside transformer core. The variation between the predicted ~23Vs peak and the measured ~26Vs peak are remarkably close and independent of the simulation tools.

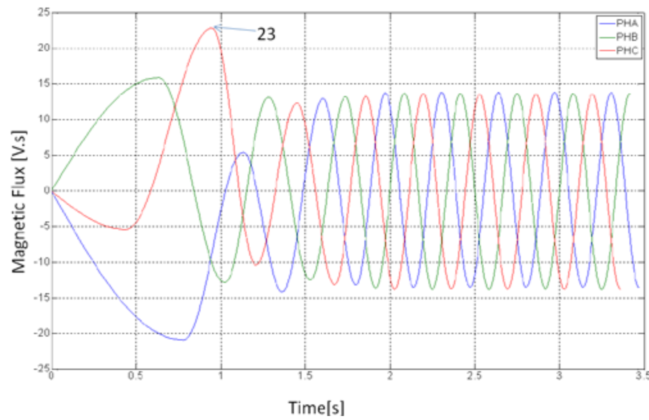

Figure 13
Topside transformer: Magnetic flux density model with the bias component mitigator applied for time > 1.2 sec

Test Results

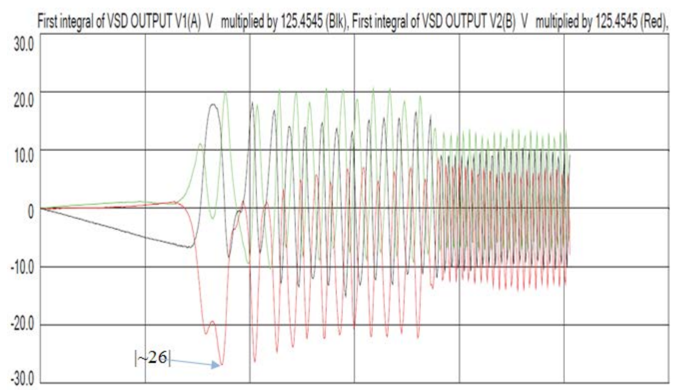

Figure 14
Topside transformer: Start-up magnetic flux density Leeds test results without bias component mitigator

Notes:
1) The voltage integration processing applied by DDS mitigates the constant component bias, while the data processed in Figure 13, from the voltage measurements, does not include this corrective factor. We do not assume that the end results regarding the peak magnetic fluxes are affected.

2) The start-up process is based on an injected ramp current in the power system. The initial magnetic flux is, therefore, independent of the post-transient, stabilized, current settings. This explains the mismatch between the high frequency peak-to-peak values in Figures 13 and 14. The maximum peak values are, however, defined by the same initial current ramp for the simulation and for the test.

Magnetic Flux Densities across Transformers

The peak values of the magnetic flux are independent of the initial rotor position, and the tests performed validate the boosting factor set by the simulation leading to an overall flux density factor below 2. It has to be noted that this factor is a resultant of the usage of a set of two transformers rated at 10 MVA for a 3.2MVA motor.

Figure 15 represents the ratio (boosting factor) between the maximum flux density obtained from a family of different start-up initial angles, and the flux density value for stabilized (post-transient) operation.

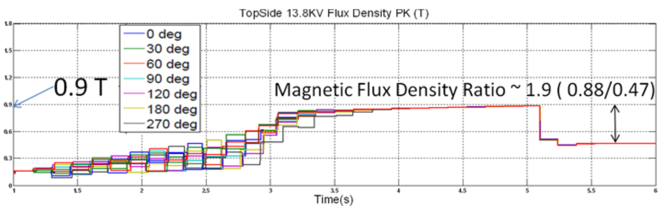

Figure 15
Topside transformer: Start-up magnetic flux density profile family for multiple initial rotor positions

CONCLUSIONS

An electric motor-driven pump system in the subsea arena proves to be an effective, power dense system with high flexibility in remotely increasing oil and gas production. The operation of a large 3MW permanent magnet motor-driven pump system, by design, improves system efficiency and reliability that lowers operator costs. Subsea electrical system design and motor performance must be predictable and validated prior to deployment.

As predicted by the test simulations discussed in this paper, a permanent magnet motor-driven pump can be remotely started and successfully controlled. In addition, it can be concluded that peak magnetic flux densities occurring in step up or step down transformers are virtually independent of either the permanent motor rotor position, or the type of motor start-up algorithm implemented.

It is important, as testing proves, that during start-up a permanent magnet motor-driven pump system does not require more electrical energy than a conventional induction motor-driven pump system. Elements such as a successful remote start-up increase confidence in the overall reliability of the system, decreasing the maintenance and intervention historically found in traditional subsea machinery. This provides a significant cost-saving benefit for subsea operators.

It should be highlighted that the potential motor start-up oscillations do not impact the sizing of the system transformers. Notably, the motor start-up profile is based on a current ramp which is independent of the rotor position.

Finally, the “Fingerprint” motor tests validated the original predictions that the maximum current required to start a permanent magnet machine is virtually independent of the initial rotor position and its potential start-up oscillations. Based on these findings, it has been predicted and now validated that the magnetic flux in the transformers’ core is independent of the initial rotor position as well.

ACKNOWLEDGEMENTS

The authors want to express their gratitude to the larger team, including FMC Technologies, Norway, Sulzer Pumps Ltd., and Direct Drive Systems, that contributed to these successful results. The simulation models were executed under FMC Technologies’ R&D programs. A special thanks to Mr. Robert Perry, Director of Subsea Processing, for his technical support and commitment in building such a diverse team.

NOMENCLATURE

A	= Transformer’s core surface [m^2]
ASD	= Adjustable speed drive – also known as Drive
BF	= Boosting factor, the ratio increase of the magnetic flux in a transformer core connected between a drive and a long line
DDS	= Direct Drive Systems, an FMC Technologies Business unit
N_{HV}	= number of winding turns on the transformer’s high voltage side
N_{LV}	= number of winding turns on the transformer’s low voltage side
PMSM	= Permanent magnet synchronous motor
RMS	= Root mean square

REFERENCES

[1] Ulvestad, H. B., et all, *Long-Step Start-Up Simulations for High Speed Permanent Magnet Motors in Subsea Operations*, IGTE 2012, Graz, Austria, 2012

[2] Ifrim, C., et all *Copper Losses and temperature Distribution in the Slots of a Liquid Filled, High Speed Permanent Magnet Motor*, IGTE 2012, Graz, Austria, 2012

[3] Cheng, S., Ifrim, C., *Long step sensorless control of permanent magnet synchronous machines with extended Kalman filter*, SLED 2012

[4] Richter, R., *Elektrische Maschinen*, Verlag Birkhaesuer, Basel, 1951.

[5] Morse, P. M., Feshbach, H., *Methods of Theoretical Physics*, McGraw-Hill, 1953